

CHAPTER 179

INTERFACIAL INSTABILITY IN STRATIFIED FLOW

by

Richard H. French*

I. INTRODUCTION

When heated water from a thermal power plant is discharged onto the free surface of an estuary or river, a density stratified flow consisting of superposed layers of hot and cold water is established. Such a flow is characterized by an initially stable interface at which there is zero velocity difference and a decaying density difference. Since it is known that after the density difference has decayed sufficiently the interface will be destroyed by turbulent eddies generated at the bottom boundary, it is pertinent to inquire if the point of interfacial stability can be easily located. It is the purpose of this paper to examine the question of interfacial stability in the presence of boundary generated turbulence and in the absence of interfacial shear.

Although the problem of interfacial stability has been previously investigated, scant attention has been given to the case of a two layer flow without shear in the presence of boundary generated turbulence. Keulegan (1949) investigated a turbulent current of fresh water moving over a quiescent pool of saline water. He concluded that the stability of the interface could be adequately described by a single dimensionless parameter, the "Keulegan" number:

$$K'_u = \frac{\bar{u}^3}{\nu g \frac{\Delta\rho}{\bar{\rho}}} \quad (1)$$

where \bar{u} is the mean velocity of the upper layer and since the lower layer was at rest, \bar{u} is also the velocity difference across the interface, ν the kinematic viscosity of the lower fluid, $\Delta\rho$ the density difference across the interface, $\bar{\rho}$ the density of the upper, flowing fluid, and g the local acceleration of gravity. Interfacial instability was defined as the point at which the rate of mixing suddenly increased; the critical value of K'_u was found to be 180.

Maxwell, et al (1975) studied arrested thermal wedges and arrested cold water intrusions. They concluded that for arrested thermal wedges an increase in bed roughness caused a corresponding increase in the interfacial friction factor; but in the case of arrested cold water intrusions changes in bed roughness had no effect on the interfacial friction factor. Although others have investigated the problem of interfacial instability; e.g., Sherenkov (1971) and

*Assistant Professor, Hydraulic and Water Resources Engineering, Vanderbilt University, Nashville, Tennessee.

Plate and Friederick (1975), the results have not been conclusive.

In the case of Keulegan's investigation, the critical value of K' should not be viewed as a constant; rather, it is a variable dependent not only on fluid viscosity but also on the turbulence present in the two fluids. Turner (1973, p. 118) has indicated that boundary generated turbulence may cause an interface to become wavy; a condition which leads to interfacial instability at values of K' substantially lower than Keulegan's critical value. Plate and Friederick (1975) have noted that field data demonstrates that in some cases buoyant plumes from thermal power plants are not observed upstream of the outlets even though the densimetric Froude number for the flow is less than one. Destruction of the interface by boundary generated turbulence could account for these observations.

The conclusions of Maxwell, et al (1975) verifies the conclusions of Turner (1973, p. 116-118) regarding the mechanisms of mixing in stratified flows. For an arrested thermal wedge, the mixing is controlled by turbulence generated at the bottom boundary, while in the case of an arrested cold water intrusion, the lower layer is stationary relative to the bottom and no turbulence is generated at the boundary. In the former case, boundary generated roughness is important while in the latter case it is unimportant.

Although these previous investigations have aided in understanding the mechanisms of turbulence generation in layered, stratified flow, they have dealt with arrested wedges rather than the environmentally important case of discontinuous vertical density profiles and continuous vertical velocity profiles. In this case, there is no shear at the interface, and interfacial stability is dependent on the stratification and the turbulence generated at the bottom boundary. In the particular case of a decaying density difference across the interface, an interface which is initially stable may at some point become unstable; and, presently, the literature offers no practical criterion for determining the point of instability.

II. EXPERIMENTS

The experiments for this research were performed in a glass flume 12.2 meters long, 1.2 meters deep, and 0.4 meters wide at the Richmond Field Station of The University of California, Berkeley. The experimental apparatus is shown schematically in Figure 1. The upstream end of the flume was connected to a mixing chamber into which fresh and saline water were injected by diffuser pipes. At the downstream end, there was a vertical slotted weir.

Saline water was injected at the entrance beneath the splitter plate by a 15.2 cm. diffuser pipe which was connected to a constant head tank. This water, which originated in San Francisco Bay, was first pumped to a holding pond (capacity 378 cubic meters), and from the holding pond to the constant head tank. The maximum sustainable saline water flow rate was 0.028 m³/s. Fresh water, supplied by a 10.0 cm. city water main to the fresh water constant head tank, was injected above the splitter plate by a diffuser identical to the one used for the saline water. The maximum sustainable fresh water flow rate was 0.071 m³/s. Within the mixing chamber directional vanes and fine mesh screening were used to damp initial turbulence. Additionally, the walls of the chamber and contracting

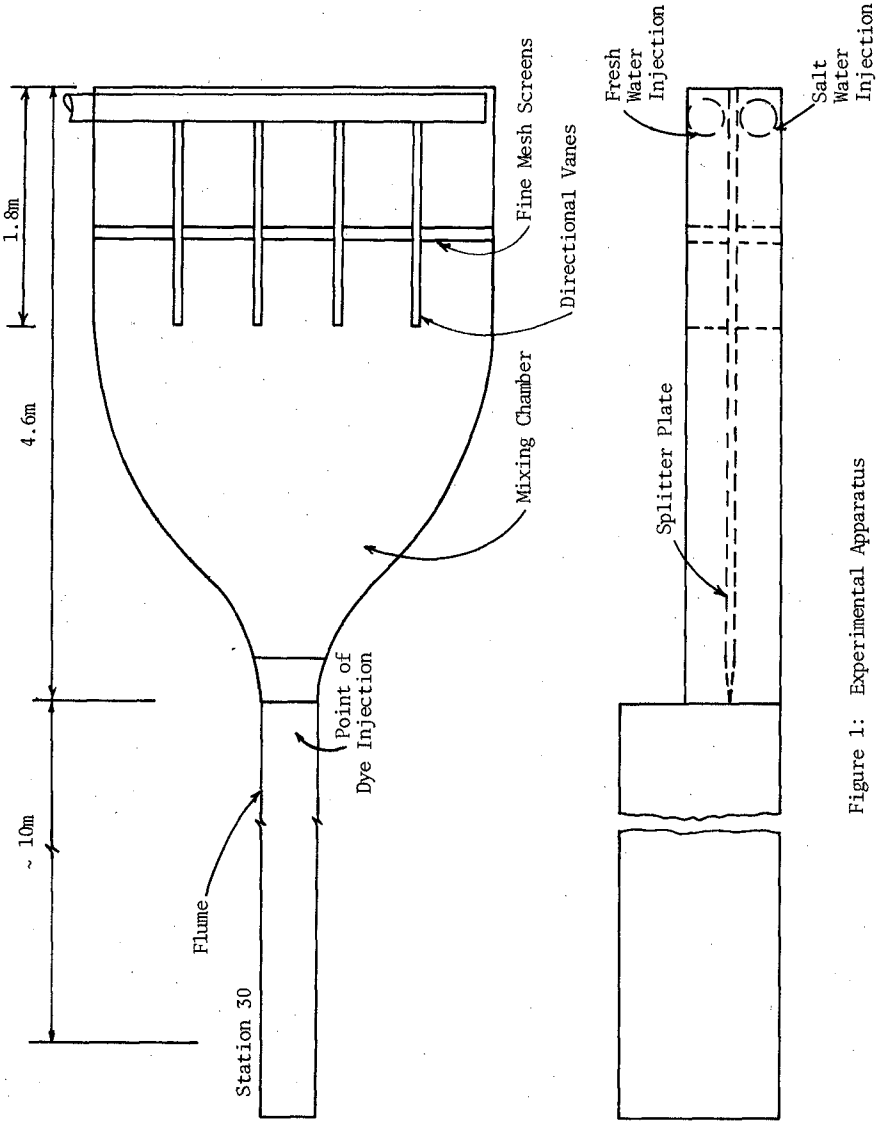


Figure 1: Experimental Apparatus

section were brought to glass like smoothness by repeated applications of epoxy paint.

Once a steady flow was established, the fresh water layer was dyed at the flume entrance to identify the position of the interface. At Station 30, ten meters downstream of the flume entrance, a visual determination of interfacial stability was made, and the results were documented by photographing the interface. The photographs were taken with a Hasselblad 500 EL camera using a Zeiss Distagon wide angle lens ($f = 50$ mm.). In addition, vertical salinity and velocity data were gathered at Station 30, and the water surface slope was determined.

Velocities were measured by a pitot-static tube connected to a PACE P7D differential pressure transducer, and the amplified signal of the transducer was recorded on a strip chart for later analysis. A vacuum system attached to the pitot-static tube was used to collect water samples, and the conductivities of these water samples were determined with a Beckman RC-19 conductivity bridge. The conductivities were converted to salinities by interpolation in a table relating temperature and conductivity to salinity, Tiphane (1962); the salinities were converted to densities by the empirical formulas of Eckart (1958).

The bottom boundary shear velocity, u_* , which was considered a direct measure of the turbulence generated at the bottom boundary, was computed by

$$u_* = \sqrt{gRS_f} \quad (2)$$

where R is the hydraulic radius and S_f the slope of the energy grade line. Since the bottom of the flume was horizontal, S_f was taken as the slope of the free surface. Although the sides of the flume were glass, the bottom was roughened by placing angular stones, approximately $2.5 \times 1.2 \times 1.2$ cm, by hand in a single layer of uniform surface height. The value of u_* calculated by Equation (2) was adjusted by the method of Vanoni and Brooks (1957) to account for the fact that the boundary roughness was not uniform; i.e., while the bottom boundary was hydraulically rough, the side walls were hydraulically smooth.

A wide range of depths and salinities were used; the input salinity was limited to a maximum of 20 ‰, because the source of the saline water was San Francisco Bay which never became more saline. The minimum salinity was 2 ‰ because at lower salinities the mixing was so strong that the flow quickly became homogeneous.

III. EXPERIMENTAL RESULTS

Before describing the experimental results, three terms must be defined in the context of this research.

Stable Interface (Figure 2): A density interface between two homogeneous fluids of different densities across which little or no mixing takes place. In Figure 2, the interface is seen as a sharp line crossed by no noticeable eddies. In this situation, the interface will remain sharp, and the flow will remain layered.

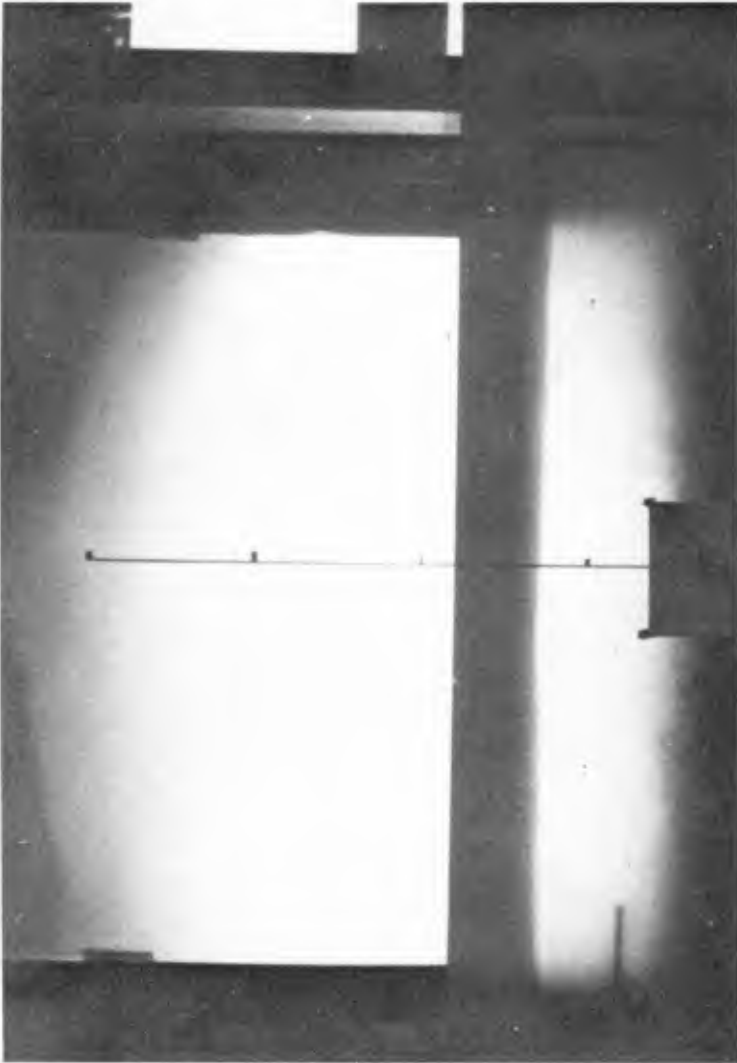


Figure 2: Stable Interface

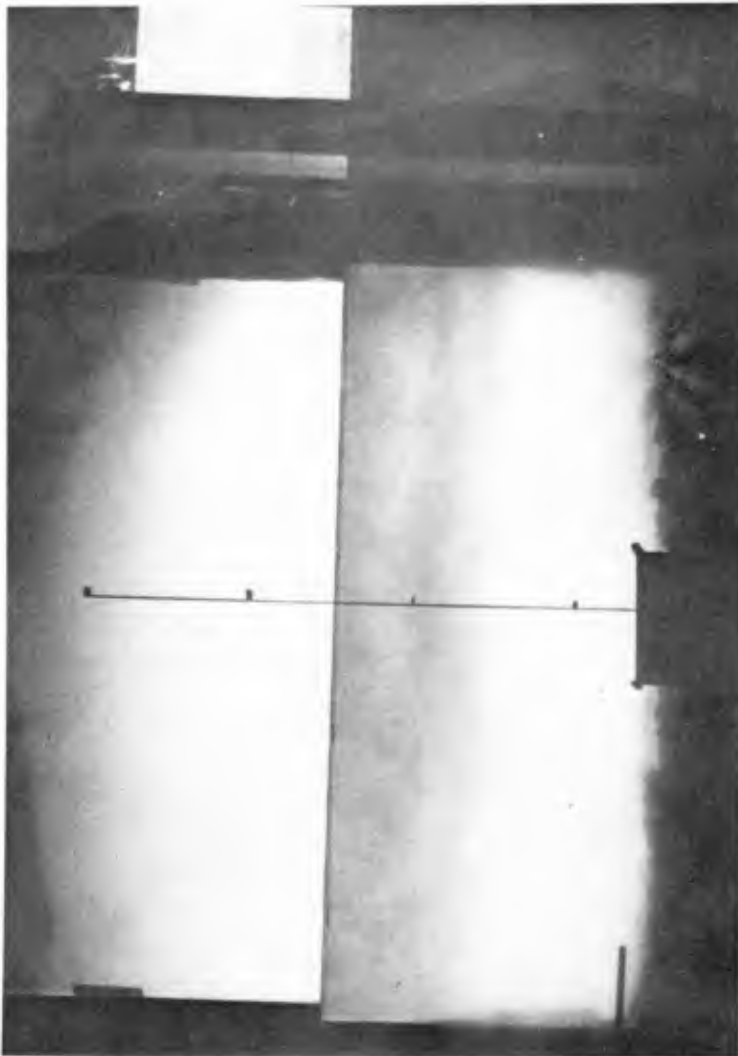


Figure 3: Unstable Interface

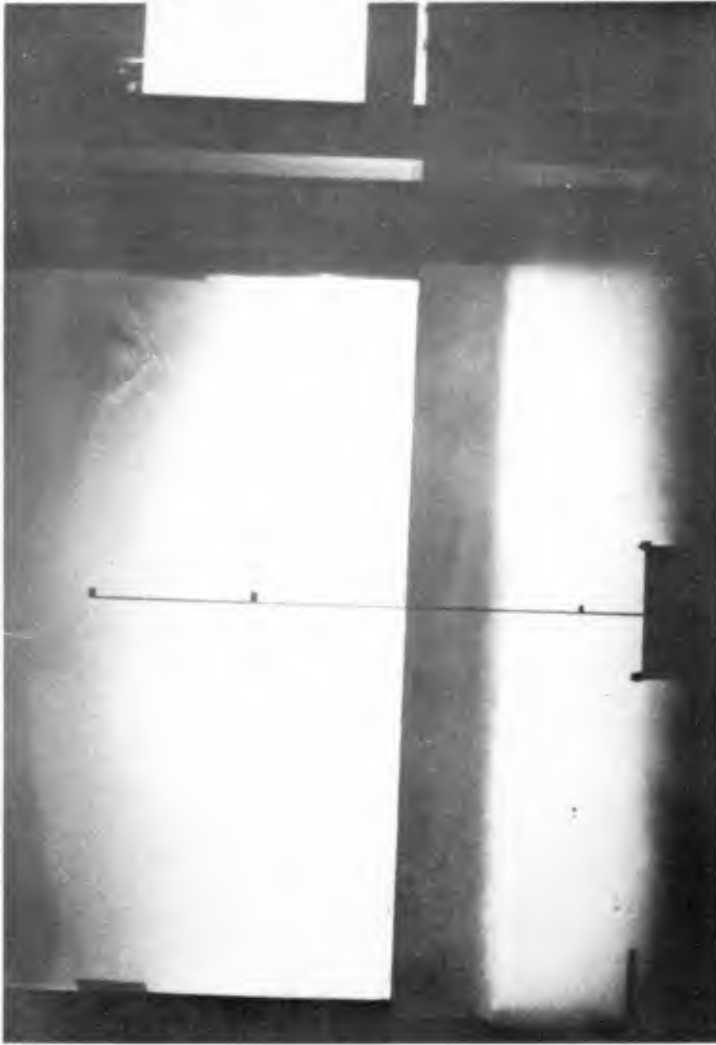


Figure 4: Transition Interface

Unstable Interface (Figure 3): This term specifies a density interface across which there is active mixing. In Figure 3, there are large, violent eddies crossing the interface in both directions; and after a finite period of time, the sharp interface will be destroyed and a continuous system of stratification established.

Transition Interface (Figure 4): This term specifies the case where the interface can be considered neither stable nor unstable. In Figure 4, although there are eddies crossing the interface, they are neither as large nor as violent as those in Figure 3; and it is not clear that the turbulence is of sufficient magnitude to completely destroy the interface.

It was assumed that in a stratified, two layer flow where the turbulence was primarily generated at the bottom boundary the stability of the interface was a function of (u_* , \bar{u} , D , $g \frac{\Delta\rho}{\rho}$, ν) where u_* is the corrected bottom boundary shear velocity, \bar{u} the average velocity of the flow, D the total depth of flow, g the acceleration of gravity, $\frac{\Delta\rho}{\rho}$ the maximum change in density across the flow, $\bar{\rho}$ the average density of the flow, and ν the kinematic viscosity of the flow. From this array of variables, the Buckingham Π - theorem states that three dimensionless groups can be formed:

$$R_o = \frac{g \frac{\Delta\rho}{\rho} D}{u_*^2} \tag{3}$$

$$K_u = \frac{\nu g \frac{\Delta\rho}{\rho}}{\bar{u}^3} \tag{4}$$

and

$$\frac{u_*}{\bar{u}} \tag{5}$$

R_o is the ratio of the fractional change in buoyancy across the flow and the depth of flow to the turbulent energy generated at the bottom boundary. As defined by Equation (4), the Keulegan number, K_u , is the inverse product of a Reynolds number, $RR = \frac{\bar{u}D}{\nu}$, and a densimetric Froude number, $FF_D^2 = \frac{\bar{u}^2}{g \frac{\Delta\rho}{\rho} D}$; i.e.,

$$K_u = \frac{1}{RR FF_D^2} \tag{6}$$

TABLE I
Experimental Data Summary

Run No.	$\bar{\rho}$ gm/cm ³	$\Delta\rho$ gm/cm ³	D cm	\bar{u} cm/s	u_{*b} cm/s	R_o	$K_u \times 10^6$	f_w	f_b	Class.
6/11/1	1.01095	0.00332	36.0	19.7	2.9	13.6	2.2	0.02	0.18	U
6/11/3	1.01095	0.00540	43.8	12.1	3.4	19.8	15.9	0.03	0.63	U
6/11/4	1.01064	0.00488	50.2	27.9	4.4	12.2	1.2	0.02	0.20	U
6/11/5	1.00976	0.00547	53.8	28.5	3.3	27.8	1.2	0.02	0.10	U
6/11/6	1.00995	0.00502	46.4	31.7	3.6	17.8	0.8	0.02	0.10	U
6/11/7	1.01019	0.00511	41.7	22.2	3.1	21.9	2.4	0.02	0.15	U
6/11/8	1.00989	0.00512	38.0	19.6	3.6	14.9	3.6	0.02	0.26	U
6/12/1	1.01179	0.00938	31.7	14.4	3.4	25.7	16.3	0.03	0.43	U
6/12/2	1.01362	0.00948	27.1	9.0	2.2	51.2	66.7	0.03	0.47	U
6/12/3	1.01439	0.00963	34.2	16.3	3.4	26.9	11.6	0.03	0.36	U
6/12/4	1.01331	0.01012	40.6	11.6	2.6	57.1	34.3	0.03	0.41	S
6/12/5	1.01249	0.01085	44.0	17.3	1.6	175.9	11.1	0.02	0.07	S
6/12/6	1.01236	0.01053	46.6	24.0	2.4	81.1	4.0	0.02	0.08	S
6/12/7	1.01327	0.01036	49.5	24.1	3.9	32.3	3.6	0.02	0.21	S
6/13/1	1.01623	0.01288	41.9	15.3	2.6	78.2	18.5	0.02	0.22	S
6/13/2	1.01379	0.01278	47.5	24.7	3.2	57.0	4.4	0.02	0.14	S
6/13/3	1.01391	0.01254	54.0	28.8	4.5	31.7	2.7	0.02	0.20	S
6/13/4	1.01392	0.01221	56.6	33.9	4.5	33.5	1.6	0.02	0.20	S
6/13/5	1.01343	0.01311	45.7	29.8	4.6	26.9	2.6	0.02	0.14	U
6/13/6	1.01447	0.01354	40.5	27.3	2.9	64.7	3.4	0.02	0.09	U
6/13/7	1.01555	0.01161	35.5	19.3	2.9	46.6	8.3	0.02	0.18	T
6/13/8	1.01568	0.01305	33.9	17.6	1.4	218.1	12.4	0.02	0.05	T
6/13/9	1.01627	0.01366	31.2	15.7	2.2	83.5	18.1	0.02	0.16	T
6/13/10	1.01126	0.00125	23.1	14.8	1.9	7.5	2.0	0.03	0.14	S
6/14/1	1.01257	0.01045	47.1	20.8	2.6	72.7	5.8	0.02	0.12	U
6/14/2	1.01326	0.00983	51.3	18.5	4.2	28.3	7.9	0.03	0.40	S
6/14/3	1.01282	0.00952	54.2	20.0	4.8	21.5	6.0	0.03	0.47	T
6/14/4	1.01290	0.00956	38.7	21.7	2.3	67.7	4.7	0.02	0.09	T
6/14/5	1.01231	0.00958	35.2	18.6	2.9	38.3	7.5	0.02	0.20	T
6/14/6	1.01203	0.00769	30.0	10.5	1.6	93.1	33.1	0.03	0.18	S

TABLE I
(Continued)

Run No.	$\bar{\rho}$ gm/cm ³	$\Delta\rho$ gm/cm ³	D cm	\bar{u} cm/s	U_{*b} cm/s	R_0	$K_u \times 10^6$	f_w	f_b	Class.
6/15/1	1.01120	0.00691	45.6	23.3	2.4	51.3	2.8	0.02	0.09	T
6/15/2	1.01200	0.00692	41.9	13.8	3.0	30.2	13.4	0.03	0.39	T
6/15/3	1.01158	0.00586	39.3	11.5	2.6	33.1	19.7	0.03	0.41	S
6/15/4	1.01158	0.00586	42.1	10.9	1.8	72.2	23.2	0.03	0.23	S
6/15/5	1.01142	0.00611	39.2	9.2	1.8	72.4	39.8	0.03	0.30	S
6/15/6	1.01094	0.00597	49.0	12.0	2.9	34.0	17.4	0.03	0.46	S
6/15/7	1.01173	0.00588	45.6	13.4	1.8	80.2	12.5	0.02	0.14	S
6/15/8	1.01115	0.00586	48.6	12.5	1.9	76.4	15.3	0.02	0.19	S
6/15/9	1.01115	0.00586	52.9	20.8	6.1	8.0	3.3	0.03	0.70	S
6/25/1	1.01573	0.01459	46.2	40.5	3.2	63.1	1.1	0.02	0.05	U
6/25/2	1.01606	0.01427	38.4	29.8	2.0	133.5	2.7	0.02	0.04	U
6/25/3	1.01503	0.01450	34.7	25.8	2.0	117.8	4.3	0.02	0.05	T
6/26/1	1.00960	0.00357	44.1	18.7	2.6	23.5	2.8	0.02	0.15	U
6/26/2	1.00940	0.00362	39.2	13.4	1.7	48.8	7.6	0.02	0.12	T
6/26/3	1.00942	0.00357	38.1	11.0	1.7	44.6	13.6	0.03	0.19	S
6/26/4	1.00966	0.00264	29.5	17.0	3.2	7.4	2.7	0.03	0.28	U
6/26/6	1.00979	0.00032	20.7	13.7	0.8	9.5	0.6	0.02	0.03	U
6/26/7	1.01015	0.00361	39.5	6.6	1.9	39.6	63.1	0.03	0.62	S
6/26/8	1.01018	0.00362	45.8	13.8	2.7	21.6	7.0	0.03	0.30	T
7/26/1	1.01080	0.00497	41.0	19.3	2.4	33.5	3.5	0.02	0.13	T
7/26/2	1.01040	0.00512	47.5	20.8	3.3	21.3	2.9	0.02	0.21	U
7/26/3	1.01040	0.00437	33.2	21.6	1.2	94.6	2.2	0.02	0.03	T

The experimental data are tabulated in Table 1. It should be noted that in most cases the friction factor associated with the bottom, f_b , was substantially larger than the friction factor associated with the glass walls, f_w . It is also noted that f_b varied over a wide range of values, apparently as a function of the Reynolds number; however, the correlation between f_b and R is very low. Thus, it is hypothesized that the variation in f_b must be either due to random experimental error or the effects of the stratification.

Interfacial stability is plotted in Figure 5 as a function of R_b and K_u . In this figure, the "line" delineating the zone of unstable interfaces from the zone of stable interfaces -- the line is the zone of transition interfaces -- is well-defined and slopes downward from left to right. In addition, three points extracted from field data gathered by Motz and Benedict (1971) downstream from the Widows Creek (Alabama) Steam Plant are plotted. The first point is near the point where the thermal plume enters the Tennessee River, and the third point is approximately one mile downstream. Point one clearly represents either a stable or transitional interface and at point three sufficient heat has been lost that the interface is unstable.

Figure 6 demonstrates the dependence of the results on the parameter $\frac{u^*}{\bar{u}}$; i.e., the data plotted in Figure 5 consists of a family of curves with a separate curve for each value of $\frac{u^*}{\bar{u}}$. In Figure 6, small values of $\frac{u^*}{\bar{u}}$ are seen to correspond to relatively large values of K_u , and large values of $\frac{u^*}{\bar{u}}$ correspond to small values of K_u . Thus, the zone of transition interfaces is a band intersecting the $\frac{u^*}{\bar{u}}$ curves.

IV. CONCLUSION

When the bottom boundary is the primary source of turbulence, Figure 5 demonstrates that it is possible to classify the stability of density interfaces between homogeneous fluids on the basis of two dimensionless parameters, R_b and K_u . This system includes the densimetric Froude number, which has previously been the sole criteria of interfacial instability, and a term which accounts for the generation of turbulence at the bottom boundary. Field verification of the results presented here is presently being sought, and it is hoped that once this is accomplished these results will be of use in analyzing the effects of non-conservative stratifying agents discharged into the environment.

Figure 5: Interfacial Stability as a Function of K_u and R_o

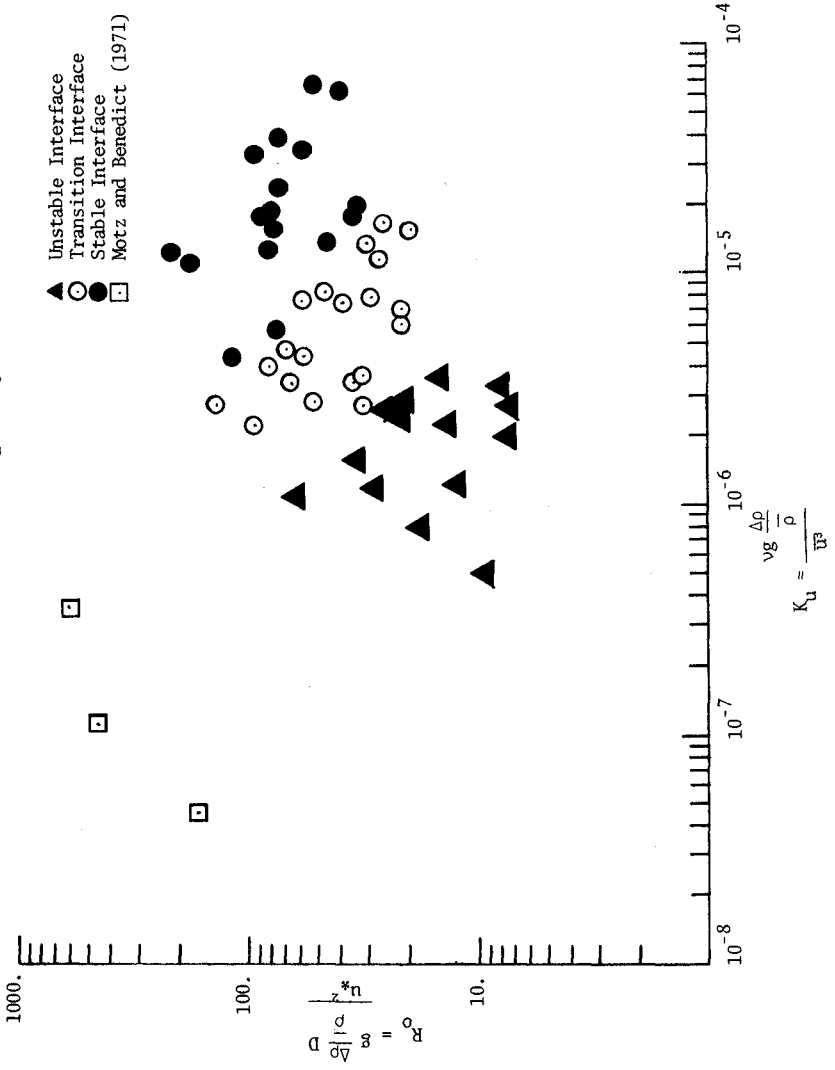
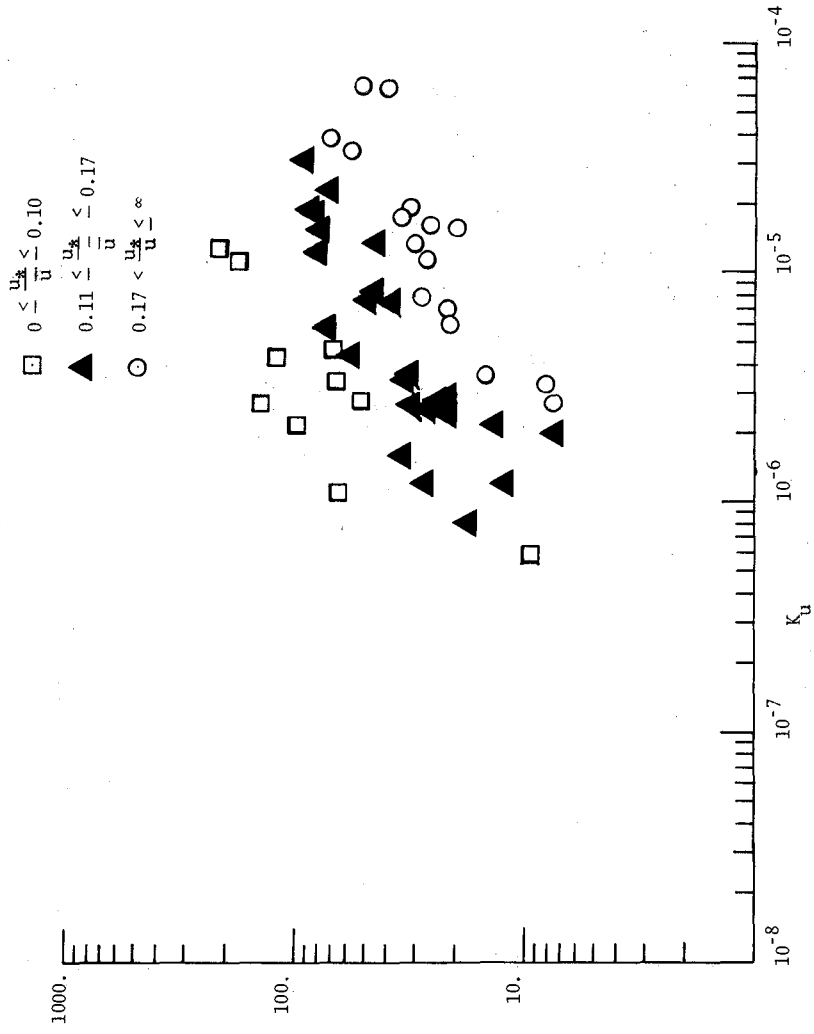


Figure 6: Dependency of Interfacial Stability on $\frac{u_*}{u}$



REFERENCES

- Eckart, Carl, "Properties of Water II - The Equation of State of Water and Sea Water at Low Temperatures and Pressures," American Journal of Science, Vol. 256, April, 1958, pp.225-240.
- Keulegan, G.H., "Interfacial Instability and Mixing in Stratified Flows," Journal of Research of National Bureau of Standards, Vol. 43, November, 1949, pp.487-500.
- Maxwell, W.H.C., Holley, E., Lin, Chi-Yu and Tekeli, Sahin, Study of Stratified Overflows and Underflows, University of Illinois at Urbana-Champaign Water Resources Center, Research Report No. 98, February, 1975.
- Motz, L.H. and Benedict, B.A., "Heated Surface Jet Discharged Into a Flowing Ambient Stream," Water Pollution Control Research Series, U.S. Environmental Protection Agency, 16130 FDQ, March, 1971.
- Plate, E.J. and Friedrich, R., "The Stability of an Interface in Stratified Channel Flow," Proceedings of the XVth Congress of the International Association for Hydraulic Research, Sao Paulo, Brazil, 1975.
- Sherenkov, I.A., Netzkarlo, A.P., and Telezhken, E.D., "Research Investigation of Transfer Process in Two Dimensional Stratified Flow," Proceedings of the XIVth Congress of the International Association for Hydraulic Research, Paris, France, 1971.
- Tiphane, Marcel and St. Pierre, Jacques, "Tables for Sea Water Salinity Determination by Electrolytic Conductivity," Faculte' des Sciences, Universite' de Montreal, Montreal, Quebec, Canada, April, 1962 (also issued as Beckman Publication No. 29.067D).